JOURNAL OF PROPULSION AND POWER
Vol. 13, No. 6, November–December 1997

Laser-Induced Spark Flameholding in Supercritical, Subsonic Flow

Lara D. Medoff*
U.S. Air Force Space and Missiles Systems Center, El Segundo, California 90245
and
Andrew McIlroy†
The Aerospace Corporation, Los Angeles, California 90009

Laser-induced spark flameholding was demonstrated, and the effect of flow and optical parameters on the flameholding distance was investigated. A pulsed Nd:YAG laser was used to induce electrical breakdown in a flow and ignite a methane/air gas mixture. The laser energy, pulse frequency, and methane concentration were varied, and the flameholding distance as a function of these parameters was determined. Results were then compared to calculated values. For a flow speed of approximately 110 cm/s and a laser repetition rate of 15–20 Hz, the flameholding distance, defined as the downstream distance from the spark to the position where continuous combustion is achieved, was found to be on the order of a few centimeters. Experimental results were extrapolated to determine the pulse frequencies required for flameholding at hypersonic flow speeds. The potential application of solid-state, continuous-wave lasers to spark flameholding is also considered.

Nomenclature

c_p = specific heat at constant pressure
E_{laser} = laser energy
E_s = stabilization energy
E_{spark} = spark energy
f_p = laser pulse frequency
$\bar{k}$ = temperature-averaged thermal conductivity
k_0 = thermal conductivity at ambient conditions
Q = heating value of fuel
r_1 = radius of kernel 1
r_2 = radius of kernel 2
S_L = propagation rate of deflagration
t = time
t_{int} = time after spark 2 of flame kernel intersection
t_1 = time after spark 1
t_2 = time after spark 2
T_f = adiabatic flame temperature
T_0 = ambient temperature
u_f = flame speed
u_m = flow speed
x_{fh} = flameholding distance
$x(t_1)$ = center height of kernel 1
$x(t_2)$ = center height of kernel 2
α_0 = thermal diffusivity
ΔT = $T_f - T_0$
δ_f = flame front thickness
ρ_f = density of the deflagration
ρ_0 = density at ambient conditions

Introduction

AN increasing number of future military and civilian hybrid space launch vehicles and aircraft will require air-breathing supersonic and hypersonic flight capability. To advance high-speed atmospheric and transatmospheric flight, a variety of technological developments are required, one of the most critical being a reliable, high-performance propulsion system. As flight speed increases into the supersonic and hypersonic realm, it becomes more difficult to maintain combustion without unacceptable pressure losses, and engine flameout becomes problematic. We address one possible means of improving air-breathing propulsion performance and reliability through novel, laser-based ignition and flameholding techniques.

Aircraft combustion chambers must operate at very low inlet temperatures and pressures, and combustion must be maintained in highly turbulent, high-speed airstreams. In high-speed flight vehicles, the airspeed in the combustion chamber is supercritical because it exceeds the burning velocity, or flame speed, of the fuel/air mixture. While typical effective flame speeds are on the order of 5–8 m/s for turbulent systems, flow speeds in combustion chambers of conventional supersonic vehicles (ramjets) are close to 30 m/s, and in proposed hypersonic vehicles (scramjets) the flow speeds are over 300 m/s. To maintain combustion within the engine, a flameholding device is required to overcome the mismatch of burning and flow speed. In gas turbine combustors, recirculation, often created by jets of cool air, is used to obtain a region where the flow speed is less than or equal to the flame speed and, thus, a flame can be maintained. In ramjet combustors and afterburners, bluff bodies are most commonly placed in the flow, creating wake regions where the flame speed can match the decelerated flow speed. The primary problem with cool air jets and bluff body flameholders is that they cause stagnation pressure losses that become significant as the speed increases into the hypersonic realm. These intrusive flameholders can also lead to acoustic instabilities in the flow such as the so-called screech phenomenon. If instead, a nonintrusive flameholder could be used, then one could maintain combustion without pressure losses or other flow disturbances.

Ronney[1] has suggested that nonintrusive flameholding may be accomplished by remotely depositing laser energy (via laser-induced sparks) into the flow to maintain combustion. There are several advantages to this method, which we will call laser flameholding. First, it eliminates the drag (pressure losses) of a conventional flameholder because no obstruction

Presented as Paper 96-3133 at the AIAA/ASME/SAE/ASEE 32nd Joint Propulsion Conference, Lake Buena, FL, July 1–3, 1996.

*Captain, Space Forces Support Branch, SMC/XRT, 2430 East El Segundo Boulevard, Suite 1340. Member AIAA.

†Technical Staff Member, Mechanics and Propulsion Department; currently at Sandia National Laboratories, M/S 9051, Livermore, CA 94551-0969. Member AIAA.

is needed in the flow. Second, it allows the flexibility of flameholder placement and overall combustor design. Finally, because laser flameholding works by continuous, active reignition, it adds reliability to a super/hypersonic propulsion system by alleviating the need to decelerate in the case of blowoff.

Lasers offer an obvious remote source of energy. However, it has proven difficult to couple the laser energy efficiently into fuel/oxidizer mixtures.[1–5] Although there have been few investigations into using lasers as flameholding devices, substantial work has been done in the related field of laser ignition. Several techniques have been exploited to produce laser ignition. Infrared lasers have been used to heat gas mixtures to produce ignition.[6] Ultraviolet lasers have been used to photodissociate molecules in the gas mixture to produce radicals that can initiate combustion.[2,7] A variety of lasers have been used to create a spark for combustion initiation by resonant, i.e., laser energy equal to an atomic or molecular transition energy, and nonresonant electrical breakdown.[1] Although the first two methods have proven successful in laboratory tests, they are difficult to implement in practical devices. Both methods are linear in laser power, and thus, ignite combustible mixtures along the entire length of the beam. Therefore, they lack control of the ignition point or region. These ignition methods also require lasers and molecular transitions that are in resonance. This puts strict limits on the types of fuels and lasers that can be used. For instance, hydrogen/oxygen, a high-performance fuel/oxidizer pair, has no convenient ultraviolet, visible, or infrared transitions. Furthermore, modern high-performance, solid-state lasers typically produce radiation in the 600–1000 nm range, where there are almost no strong molecular absorptions. Laser-induced spark ignition overcomes the inherent difficulties of these other methods, and is a viable and efficient technique for practical devices.

Although laser-induced sparks have received relatively little attention as an ignition method, cathode sparks, those created by electrodes, are commonly used for combustion chamber ignition. They have not been used for flameholding because the electrode cannot reasonably be situated in the flow and cannot meet the repetition rate, material strength, and lifetime requirements. Furthermore, the electrodes themselves would protrude into the flow and act as bluff bodies. Laser-induced sparks provide several advantages over conventional electric-discharge spark sources or other laser ignition methods. Lasers allow a choice of spark location without electrodes or other physical obstructions in the flow. Because the spark formation process is highly nonlinear in energy density (typically sixth-order for a visible laser), for typical lasers, the minimum energy density needed can only be obtained at the focus of the beam. Therefore, by choosing the focal point of the laser, one can select the spark location and, thus, the flameholding location. Typically, more than 50% of the laser energy is deposited in the spark, an efficient coupling between the laser and combustion processes (see the Results section). Furthermore, because laser-induced sparks can be generated by nonresonant breakdown, their formation does not depend critically on the gas mixture or type of laser. Thus, readily available, efficient, rugged, solid-state lasers, such as high-power diode lasers, can be used for the laser sparking system. Diode lasers are relatively inexpensive and are already employed on space flight systems for ordnance ignition.

In this study, we investigate the suitability of using laser-induced sparks, generated by nonresonant gas breakdown, for flameholding applications. We experimentally investigate pulsed, laser-induced spark flameholding in low speed, supercritical flow, and analytically scale our results to laser-induced spark flameholding in a super/hypersonic flowfield. The purpose of our investigation is to demonstrate that laser flameholding via laser-induced sparks can be accomplished, and to determine the effects of flow and optical parameters on the flameholding location.

Background and Theory

Flameholding is needed in any combustor where the flow speed exceeds the flame speed. It has traditionally been defined as "creating in a high-speed gas stream, a region whose velocity is lower than the burning velocity of the mixture."[8] However, utilizing laser energy, we can achieve the same effect that traditional flameholders achieve without decelerating the gas flow. The purpose of a flameholder is to maintain combustion. Therefore, it is logical to define a flameholder simply as a device that serves this purpose. Ignition devices such as laser-induced sparks would then be included in this category.

No previous experimental work on maintaining a flame in a supercritical flow using laser-induced sparks for energy deposition is known. Fendell et al.[9] analyzed the configuration of a flame held in a low-speed supercritical flow by both continuous and intermittent laser energy sources. They showed that for a continuous-ignition point source, the flame appears conical in shape with the point of the cone at the energy deposition location. Qualitative discussion of a pulsed-ignition point source concluded that flame kernels developing from each ignition intersect to form an approximately conical flame front.

Hill and Peterson[10] showed that the conical flame front resulting from a pulsed or continuous wave (cw) spark train is similar to the effect of a bluff body. The bluff body creates a region of recirculating hot gases in its wake that acts as a continuous ignition source similar to the proposed continuous spark. The flame front then expands conically off of the body. Figure 1 shows a cartoon of spark and bluff-body flameholders. When an intermittent spark source is located in the flow stream (Fig. 1a), a series of flame kernels, spherical regions of burned gas, expand at the u_f rate (with the simplifying assumption that reactants and products have the same density and that u_f is constant), while the flame kernel centers travel downstream with u_m. When combustion is initiated by a continuous spark source (Fig. 1b), a conical region of combusted

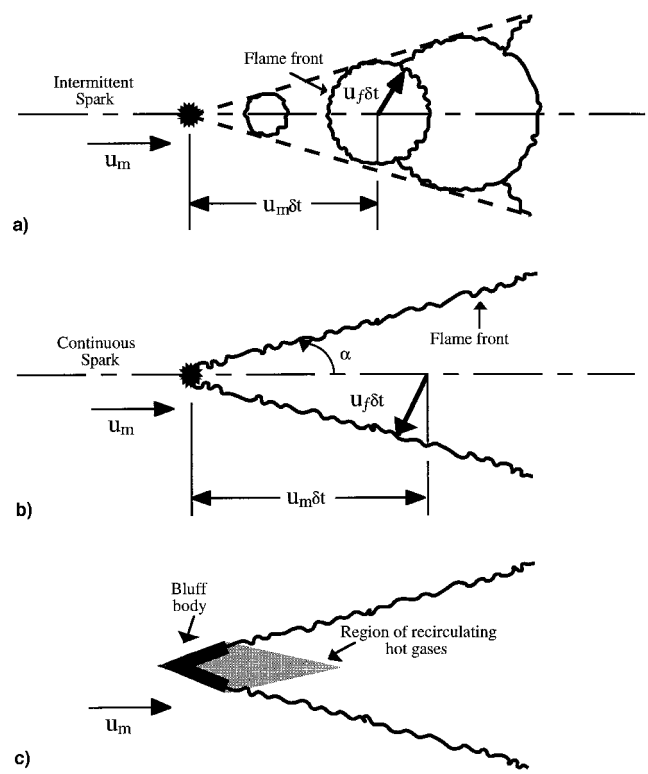

Fig. 1 Schematic representation of spark and bluff-body flameholders in a combustible mixture flowing with a uniform and parallel velocity u_m. The flame speed of the burning mixture is u_f, where $u_f < u_m$; a) combustion initiated by an intermittent spark, b) combustion initiated by a continuous spark, and c) combustion maintained by a bluff body (adapted from Hill and Peterson[10]).

material results, the cone angle being $\sin^{-1}(u_f/u_m)$. To utilize a bluff body for combustion maintenance (Fig. 1c), first, the flow must be ignited, and once ignited, the recirculation of hot gases in the wake of the body acts like the continuous spark to hold the flame. There has been a large body of experimental work on bluff-body flameholders, much of which has been summarized by Lefebvre.[8]

Although laser-induced spark flameholding has not been investigated experimentally, the mechanisms on which it is based: laser-induced electrical breakdown (sparking) and laser-induced spark ignition and flame kernel growth have received considerable laboratory attention. Raizer[2] and Morgan[12] reviewed the large body of theoretical and experimental work on the laser-induced electrical breakdown of gases. Syage and coworkers[13] investigated flame propagation initiated by laser-induced sparking in H_2/air, and Spiglanin et al.[14] imaged very early flame kernel growth for the laser spark ignition of $H_2/O_2/Ar$ mixtures.

Experimental research in laser-induced sparks has been carried out using both pulsed and cw lasers.[1] For flameholding purposes, one can use either type of laser, and each has its advantages. As we will show, practical flameholding is limited by the repetition rate for pulsed lasers and by the power requirements for the cw laser. With either laser type, however, the process of flameholding is the same. One must first create a spark, then ignite the gas, and finally, maintain the flame for an indefinite amount of time.

Spark Formation

A spark, which is simply a region of plasma, forms when the laser power density exceeds the threshold for breakdown. The density, ionization potential, and polarizability of the gas used determine this threshold. The laser-induced breakdown occurs in two stages. First, a small fraction of the interaction volume is multiphoton ionized by the laser. Second, the liberated electrons then participate in an inverse Bremmstrahlung process in which the electrons absorb additional photons during electron-neutral collisions. These energetic electrons then collisionally ionize other molecules, creating a cascade that forms the bulk of the spark. The threshold power density is on the order of megawatts/centimeters cubed (Refs. 11 and 15). Because lasers can be tightly focused, a high-power density can be achieved in a small region with relatively modest laser power. For a pulsed laser, the energy is released over a very short time frame (picoseconds, nanoseconds, or microseconds), so that the peak power is extremely high, even for low average power lasers. A 20-Hz repetition rate pulsed laser with only 1-W average power focused down to 0.1 mm can easily create a spark in air. For a cw laser focused down to less than 1 mm, the breakdown threshold is approximately 2 kW.[10] Compact, 2-kW-powered cw lasers are not yet available, which has discouraged the application of cw laser-induced sparks.

Ignition

Although spark formation can be a very rapid process, taking place in less than 10 ns, ignition is much slower, on the order of 100 μs for hydrocarbon fuels at 1 atm and 298 K. Thus, once the spark is formed, it can be viewed to zeroth-order as a heat source, and using the heat equation, one can determine if ignition takes place. Ignition will occur if the energy deposition within the critical flame kernel radius exceeds the minimum ignition energy. The radial growth of the kernel depends on the temperature rise of the gas because of energy deposition and combustion. Ronney[1] gives the minimum energy needed for ignition as

$$E_{\min} \cong \frac{4\pi}{3}\left(\frac{\alpha_0}{S_L}\right)^3 \rho_f Q \left(\frac{\bar{k}}{k_0}\right) \tag{1}$$

where $\alpha_0 = k_0/\rho_0 c_p$ and $Q = c_p(T_f - T_0)$; this holds for both pulsed and cw lasers. For stoichiometric hydrocarbon fuel/air, the minimum ignition energy is on the order of 0.2 mJ.[16]

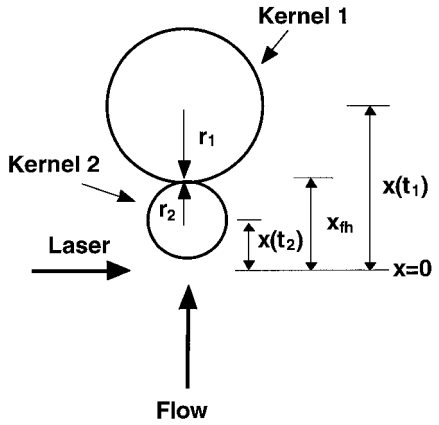

Fig. 2 Schematic representation of flameholding distance. The spark location is $x = 0$. The upper kernel is from the previous spark and the lower kernel is from the current spark.

Flame Maintenance

Once ignition takes place, a flame kernel forms, but in a supercritical flow, the flame will blowoff without further action. In pulsed laser-induced spark flameholding, each spark reignites the gas mixture, forming a series of intersecting flame kernels (Fig. 1). The flame kernels come together to form an approximately conical region of burned gas emanating from the spark. Although the spark location might be considered the site of flameholding, the critical position is where the two most recent flame kernels intersect; at this point, a continuous flame exists (Fig. 1), and the flame structure becomes similar to that of a traditional flameholder. Thus, we have defined the flameholding distance for pulsed laser-induced spark flameholding as the distance from the spark to this intersection. The flameholding distance is a function of flow speed, flame speed, and pulse frequency f_p. Ignoring buoyancy effects, and assuming independent spherical flame front propagation, we can calculate the flameholding distance by finding the point at which the flame kernels intersect (Fig. 2). If we define x_1 as the location of the lower edge of the earlier generated flame kernel (kernel 1), and x_2 as the location of the upper edge of the most recently generated flame kernel (kernel 2), then from Fig. 2

$$x_1 = x(t_1) - r_1 \quad \text{and} \quad x_2 = x(t_2) + r_2 \tag{2}$$

where $t_1 = t_2 + 1/f_p$. The distances x_1 and x_2 are expressed in terms of the flame and flow velocities as

$$\begin{aligned} x_1 &= u_m\left(t_2 + \frac{1}{f_p}\right) - \int_0^{t_2 + 1/f_p} u_f \, dt \\ x_2 &= u_m t_2 + \int_0^{t_2} u_f \, dt \end{aligned} \tag{3}$$

We have defined the flameholding distance x_{fh} to be the point of intersection of the two flame kernels, that is when x_1 equals x_2. Intersection occurs when t_2 equals t_{int}. Setting x_1 equal to x_2

$$u_m\left(t_{\text{int}} + \frac{1}{f_p}\right) - \int_0^{t_{\text{int}} + 1/f_p} u_f \, dt = u_m(t_{\text{int}}) + \int_0^{t_{\text{int}}} u_f \, dt \tag{4}$$

$$x_{\text{fh}} = u_m(t_{\text{int}}) + \int_0^{t_{\text{int}}} u_f \, dt \tag{5}$$

From Eq. (4), we can find t_{int}, and thus, x_{fh} from Eq. (5). However, this requires an expression for u_f. If we assume a

constant flame kernel expansion speed u_f, then the flameholding location is given by

$$x_{\text{fh}} = -\frac{u_f}{2f_p} + \frac{u_m^2}{2u_f f_p} \tag{6}$$

However, the flame kernel expansion rate is not constant, and no simple expression exists for u_f during initial kernel expansion.[14]

For cw laser-induced spark flameholding, the flameholding distance is at the spark because there is no gap of unburned gas after that point. To maintain the conical flame emanating from the cw spark, Ronney[1] suggests that the energy input must sustain the flame region at the flame temperature. Using this assumption, he finds that the stabilization energy E_s is

$$E_s \cong \delta_f^2 \rho_0 u_m c_p \Delta T \cong \delta_f (u_m/S_L) \bar{k} \Delta T \tag{7}$$

where δ_f^2 is the cross-sectional area of the heated region. For stoichiometric hydrocarbon fuels and a flow speed of Mach 1, this equation yields a power requirement of ~40 W,[1] well below the ~2 kW required to maintain a cw spark.[10] Thus, the most power-efficient laser-induced spark flameholding method may require the use of pulsed lasers, rather than cw lasers, to balance the peak power required for spark formation with the average power required for flameholding.

Experimental Method and Setup

To demonstrate that pulsed laser flameholding in supercritical flow is possible and to investigate the combustion dynamics of this process, images of flame kernel growth were taken at varying time delays before and after sparking. The experimental setup is shown in Fig. 3a. The sparks were created by a frequency-doubled, pulsed, Q-switched, Nd:YAG laser. The laser produced 7-ns-wide pulses at frequencies up to 20 Hz with pulse energies up to 1.0 J. Pulse-to-pulse energy variation is 10%. The laser was focused with a 50-mm focal-length lens 2.0 cm above a burner, after which a second 50-mm lens recollimated the beam. The beam waist was approximately 0.01 cm, and the laser irradiance at the waist was typically 600 MW/cm^2. Spark energies were determined by measuring the laser pulse energy before and after the spark with calibrated energy meters. The average spark energy was measured. The actual spark energy fluctuated 20% about the average value because of variations in laser energy and beam quality, which affect focusing. Losses caused by scattering of the laser off of the spark have been shown previously to be negligible compared to shot-to-shot energy fluctuations.[13] A time-gated, intensified, slow-scan charge-coupled device (CCD) camera system was used to image the CH A-X flame emission through a 430-nm Schott glass filter. The camera has a 384 × 576 pixel array with 16-bit resolution. Digital delay generators controlled camera and laser timing.

A purpose-built burner based on classical premixed, flat flame burners was constructed. The burner was designed to create a smooth, uniform, supercritical flow stream wide enough to allow for flame kernel expansion. The burner consisted of a 2.0-cm-diam core surrounded by a shroud with a 3.2 cm o.d. Premixed fuel and air flowed through the core. Nitrogen flowed through the shroud at the same flow speed as the core to minimize shear layer mixing with ambient air. Glass beads and fine mesh screens were used as flow straighteners in both the core and shroud. Figure 3b shows a shadowgraph image of an SF_6–N_2 gas mixture exiting the burner core with an N_2 shroud flow. The flow appears smooth, with a low level of turbulence. The cold-flow speed was measured with a hot-wire anemometer with a 5% accuracy, and was found to be constant within 10% up to 9 cm above the burner.

Gas mixtures and flow rates were controlled with mass flow controllers individually calibrated to each gas using a volumetric flowmeter. Flows were controlled with an accuracy of ±0.1% by volume. All gas mixtures are reported in volume percent. All experiments were performed at ambient temperature and pressure (298 K, 1.0 atm), with methane/air mixtures and nitrogen shield gas at a flow velocity between 100–115 cm/s. The time-evolution of flame kernel expansion was recorded while varying laser pulse rate, laser energy, and methane concentration. Time delays between the ignition laser pulse and image acquisition are accurate to ±1 μs. The flame kernel expansion rate and location of flame kernel intersection was measured from the images. To determine the size of the flame kernels, an image of a ruler placed at the center of the burner was recorded and used to calibrate the spatial scale of the other images. The resolution of the ruler was 0.05 cm. Four images were taken at each experimental condition, and the average of

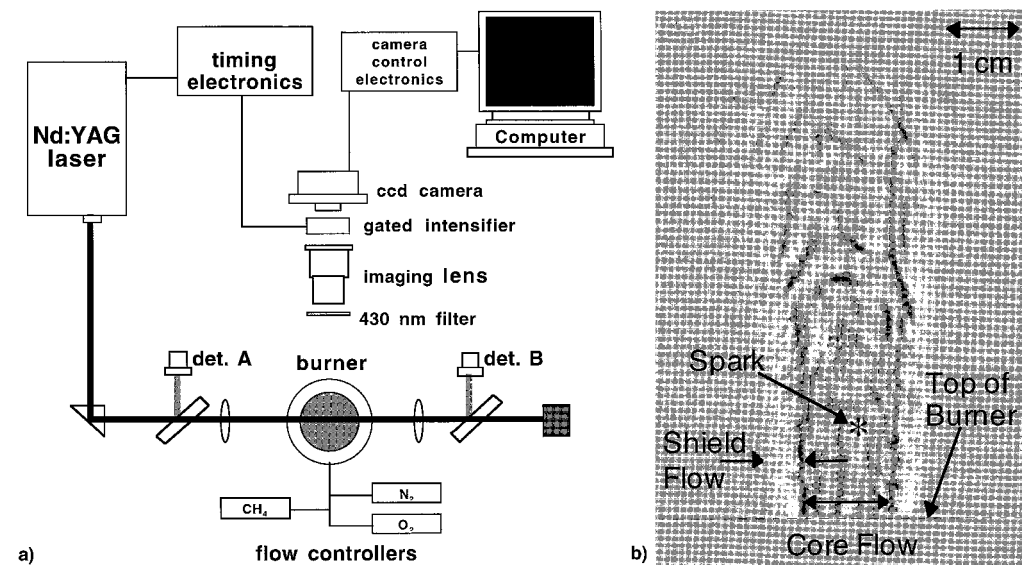

Fig. 3 a) Experimental apparatus. Nitrogen, oxygen, and methane flow through calibrated mass flow controllers, mix, and are directed into a 2.0-cm-diam burner. A frequency-doubled, pulsed, Nd:YAG laser is focused above the burner to form a laser-induced spark. To record the evolution of the flame kernels, a time-gated, intensified CCD camera system images the CH A-X emission through a 430-nm Schott glass filter. b) Shadowgraph of flow stream. Flow is smooth with low level turbulence. Sparks are formed approximately 2 cm above the top of the burner. The concentric ring pattern about halfway up the image on the left-hand side is from interference effects caused by neutral density filters. The apparent cutoff of the flow near the top of the image is because of limited camera FOV.

the four flame kernel diameters was used as the diameter for the condition. Kernel size and position variation between images was less than 10%. The location of the flame kernel intersection, i.e., the flameholding distance, was likewise found as the average of the four measured positions. The error in these measurements was typically ±10% of the distance, and resulted primarily from fluctuations in the spark energy and uncertainty in determining the position of the edge of the slightly wrinkled, curved flame front.

Results

We first describe the general features of pulsed laser-induced spark flameholding, and then the effects of varying the spark energy, laser pulse frequency, and methane concentration on the flameholding distance. We describe the general features of laser flameholding under the following typical conditions: 15-Hz laser pulse frequency, 45-mJ/pulse laser energy, and laser focus 2.0 cm above the burner. The train of laser-induced sparks ignited a 7.2%, by volume, methane/air mixture flowing out of the burner at 102 ± 5 cm/s. An apparently stable, conical flame, light blue in color, was visible to the naked eye. When the laser was removed, the flame blew off, indicating that the laser was indeed maintaining the flame. The stability of the flame was investigated using a time-gated, intensified CCD camera. Exposures of 100 μs duration were taken at various times before and after spark formation. A series of these images is shown in Fig. 4. Before the laser pulse forms the spark, the remnants of the flame kernel from the previous spark remain in the camera field of view (FOV). This flame front moves upward with a relatively constant velocity (55 cm/s), that is a balance between the upward flow velocity and the downward flame velocity. The flame speed in this case is ~45 cm/s, higher than the laminar flame speed (25 cm/s) at this methane concentration because of the wrinkling of the flame front. Shortly after spark formation, a new flame kernel, toroidal in shape, is formed and initially expands rapidly. The kernel is toroidal, rather than spherical, because the spark is elongated parallel to the laser beam, which is well known to induce a toroidal flowfield.[14] The initial expansion is rapid enough to allow the new flame kernel to overcome the flow velocity and intersect the previous flame kernel remnants 15 ms after the spark. The distance to the point of intersection from the spark location, what we have defined as the flameholding distance, was 3.8 cm in this case. We investigated the change in this distance with the variation of the input energy, laser pulse frequency, and methane concentration.

Energy Effect

To determine the effect of input energy on flameholding distance, the laser energy was varied from 22.5 to 180 mJ/pulse. The lower limit, 22.5 mJ, was determined by the minimum energy at which sparks could be consistently formed with our doughnut mode laser. Previous works[12,13] has shown that sparks can be reliably formed at much lower pulse energies with lasers whose transverse mode structure more closely approximates a Gaussian TEM_{00} mode. The upper energy limit of 180 mJ was the highest energy obtainable throughout the pulse frequency range of the laser (1–20 Hz). Only a fraction of the laser energy was absorbed by the spark and, thus, deposited in the gas. The average spark energy as a function of laser energy is shown in Fig. 5. Over the region investigated, the spark energy increased linearly with the laser energy, and was fit to the function:

$$E_{\text{spark}} = 0.735E_{\text{laser}} - 7.69 \tag{8}$$

The initial expansion of the flame kernel was found to increase with increasing spark energy. As noted earlier, the expansion was toroidal with the kernel expanding faster in the direction transverse to the laser beam axis (parallel to the flow velocity). Because flameholding takes place along this axis (the x axis), we report all flame kernel size measurements along the x axis. Figure 6 shows the x-axis diameter of the flame kernel (measured from edge-to-edge) 2.0 ms after the spark as a function of spark energy. The kernel size at 2.0 ms shows a strong, nonlinear dependence on the spark energy. The steepest dependence appears at energies below ~60 mJ, rolling off at higher energy. The spark energy affects the rate of flame kernel expansion only for the first 2.0 ms. In Fig. 7, the flame kernel diameter as a function of time is given for spark energies of 8.4, 27, and 57 mJ. For each energy, the flame kernel expands rapidly for approximately 2.0 ms before leveling off to a steady expansion rate that is independent of the spark energy. The initial expansion was found to be a function of spark energy alone, and was unaffected by changes in methane concentration. The long-time expansion rate (225 cm/s) is characteristic of a thermally-driven flame kernel and is approximately equal to $u_f(T_f/T_0) \sim 30$ cm/s (2000/300 K) ~ 200 cm/s.

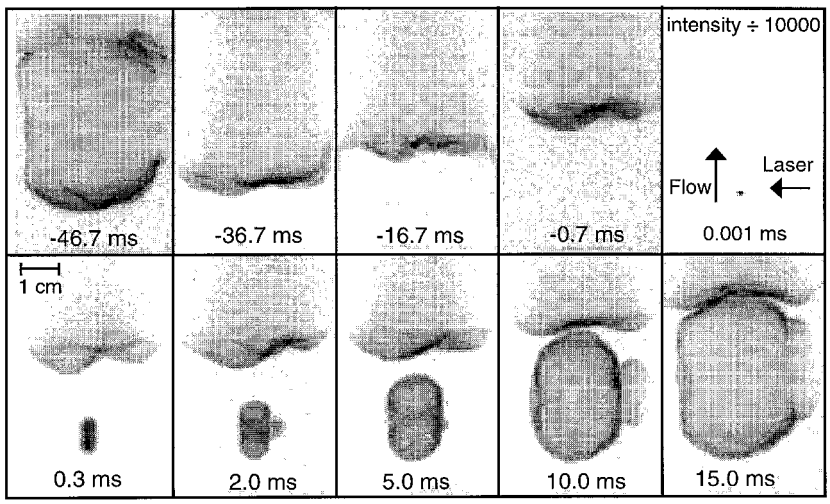

Fig. 4 CH emission images of pulsed laser flameholding. Darker areas represent a higher signal. The first panel shows the flame kernel from the previous spark. In the next three panels, the flame kernel rises at a rate approximately equal to the difference of the flow and flame speeds. In the fifth panel, the laser spark is formed. Note that the peak intensity of the spark is about 10^5 times higher than the peak intensity of the flame and, thus, the flame kernel from the previous spark is not visible. In the first panel of the bottom row, we have the flame kernel from the new spark expanding and the flame kernel from the previous spark above. In the next four frames, the flame kernel expands until it intersects the previous flame kernel in the last frame, 15 ms after the spark.

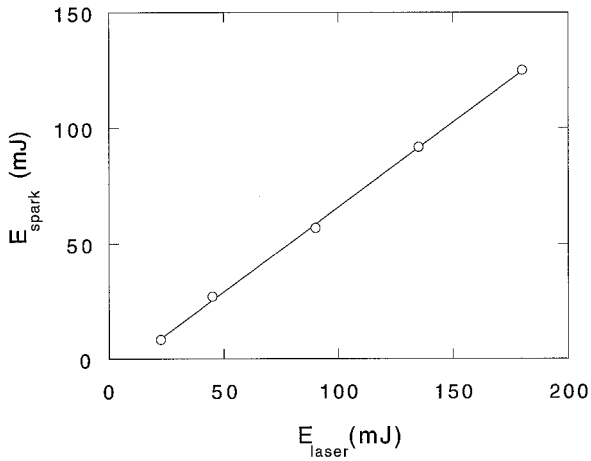

Fig. 5 Spark energy as a function of laser energy.

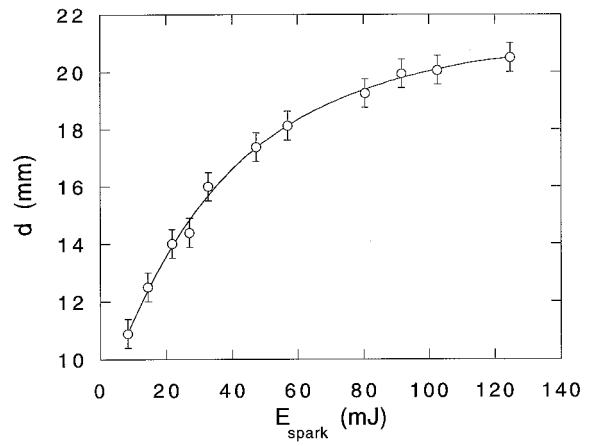

Fig. 6 Flame kernel diameter 2.0 ms after spark formation as a function of spark energy at a methane concentration of 7.2% by volume.

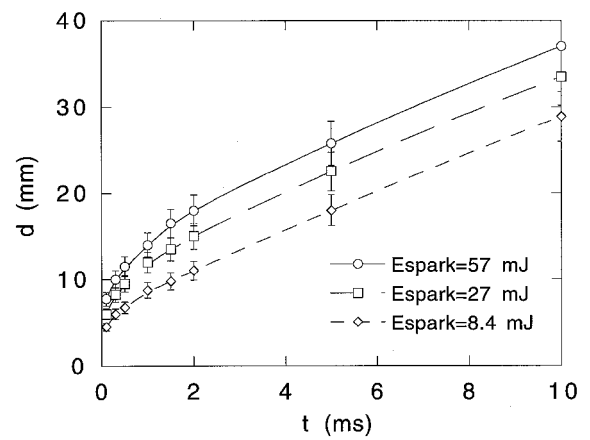

Fig. 7 Plot of the flame kernel diameter as a function of time after spark formation for three different input energy values at a methane concentration of 7.2% by volume.

A combination of adiabatic expansion of the hot gases within the kernel and propagation of the flame front drive the kernel expansion. At early times (t < 2 ms), the residual heat from the spark accelerates the propagation by contributing to the overpressure that must be relaxed by expansion and by increasing the flame speed by raising the temperature near the flame front. Beyond 2 ms, the expansion appears to be driven by the combustion process alone. The data in Fig. 6 show that the flame kernel expansion rate is less sensitive to the spark

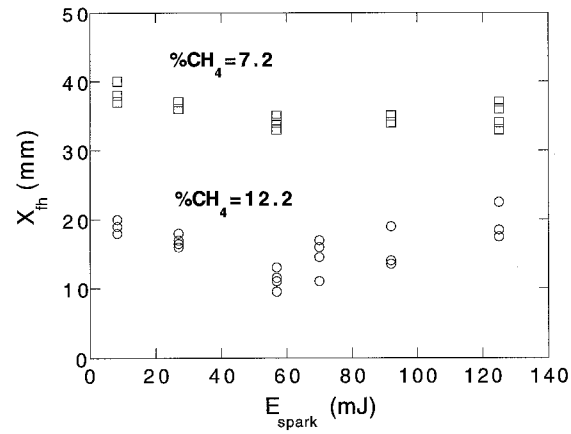

Fig. 8 Flameholding distance as a function of spark energy given for two methane concentrations. Scatter in the data is characteristic of uncertainty.

energy above ~60 mJ. The decreased sensitivity may be related to the formation of a shock wave by the spark. Because the spark energy deposition occurs in <10 ns, the spark is initially at high temperature (T > 10,000 K) and pressure (P > 20 atm). Much of the overpressure is relaxed by the formation of a shock wave. The energy carried away from the kernel by the shock wave may have a nonlinear dependence on the spark energy caused by chemical reactions occurring in the shock front.[14] Thus, at higher spark energies, more energy would be lost to the shock wave, and less energy would be available to drive the kernel expansion.

Because the flame kernel expansion rate increases significantly between spark energies of 8.4–57 mJ, we would expect the flameholding distance to decrease with increasing energy in this range. The data in Fig. 6 suggest that increasing the energy above 60 mJ would have little effect on flameholding distance. Figure 8 displays the experimental flameholding distance as a function of spark energy for methane concentrations of 7.2 and 12.2%. At both concentrations, the flameholding distance decreases as the energy increases to 60 mJ. For 7.2% CH_4, the flameholding distance then levels off. However, above 60 mJ, an increase is observed for 12.2% CH_4. This increase may be related to the stronger shock waves postulated earlier; however, a definitive understanding of this phenomenon is lacking.

For both methane concentrations shown in Fig. 8, the dependence of the flameholding location on energy is relatively weak. At 7.2 and 12.2% CH_4, the flameholding position is reached at 15 and 7 ms after the spark, respectively. In these cases, the expansion caused by combustion dominates over the spark heat-induced expansion. When the flameholding position is reached in <2 ms, the energy effect should increase in significance.

Pulse Frequency Effect

The laser pulse frequency was varied from 15 to 20 Hz. The lower limit, 15 Hz, was chosen to keep the flameholding distance in the camera FOV for all energy levels and methane concentrations. The upper limit (20 Hz) was the maximum repetition rate of the laser. Figure 9 shows the experimental flameholding distance as a function of pulse frequency along with calculated flameholding distances for three different flow velocities. The experimental spark energy was 27 mJ and the flow velocity was 112 ± 5 cm/s. The curves in Fig. 9 were calculated using Eqs. (4) and (5). Because there is no general analytical expression for the flame speed u_f,[14] especially at short times after ignition, we used our experimental data to derive an expression for the flame speed in the x direction.

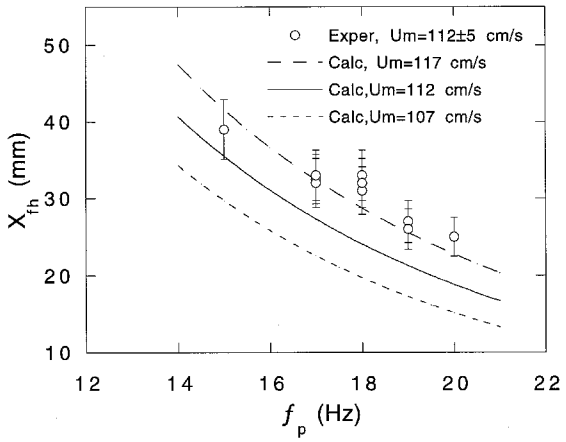

Fig. 9 Flameholding distance as a function of pulse frequency, E_{spark} = 27 mJ. The circles are experimental data taken at a flow velocity of 112 6 5 cm/s, and the curves are calculated values of a flameholding distance at three different flow velocities.

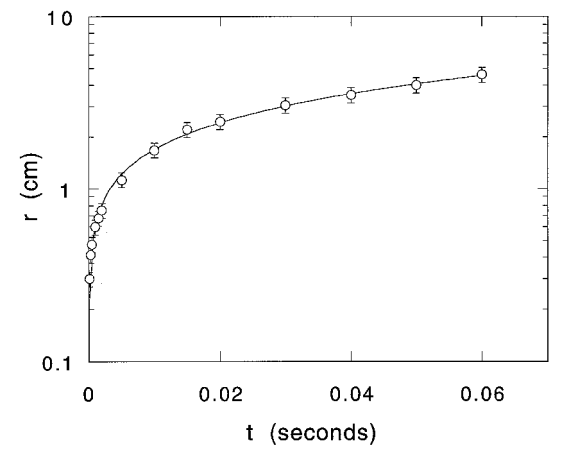

Fig. 10 Flame kernel radius as a function of time. E_{spark} = 27 mJ and % CH_4 = 7.2 by volume. The circles are the measured radius values, and the line is a curve fit to the data [Eq. (9)].

Figure 10 displays the x radius as a function of time. These data were fit to the following expression:

$$r = 8.62t^{0.393} + 28.2t \tag{9}$$

where r is in centimeters and t is in seconds. Equation (9) was differentiated with respect to time, to obtain

$$u_f = 3.39t^{-0.607} + 28.2 \tag{10}$$

where u_f is given in centimeters per second. Substituting Eq. (10) into Eqs. (4) and (5) yield the following expressions for t_{int} and x_{fh}:

$$\frac{u_m}{f_p} = 8.62[(t_{int} + 1/f_p)^{0.393} + t_{int}^{0.393}] + 56.4t_{int} + \frac{28.2}{f_p} \tag{11}$$

$$x_{fh} = (u_m + 28.2)t_{int} + 8.62t_{int}^{0.393} \tag{12}$$

where x_{fh} is given in centimeters and t_{int} is in seconds. The flameholding distance was found to be sensitive to flow velocity (Fig. 9). The data agree with the calculation, but the flameholding distance is systematically higher than the calculation for the measured flow speed, 112 cm/s. Better agreement is found with a calculation based on a flow speed of 117 cm/s, which is within the experimental uncertainty of the flow speed measurement. The discrepancy between the measured and calculated flameholding distances may be caused by either systematic error in the flow speed measurement or interactions between the flame kernels not taken into account in the model.

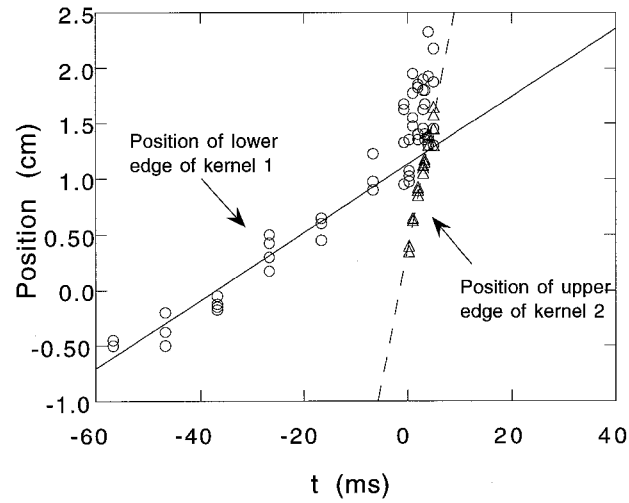

Fig. 11 Experimentally determined distance above spark location of the lower edge of kernel 1 and the upper edge of kernel 2 as a function of time after spark 2. The data were taken at a methane concentration of 12.2% by volume and a spark energy of 27 mJ (see Fig. 2 for the definition of kernels 1 and 2). Scatter in the data is characteristic of uncertainty.

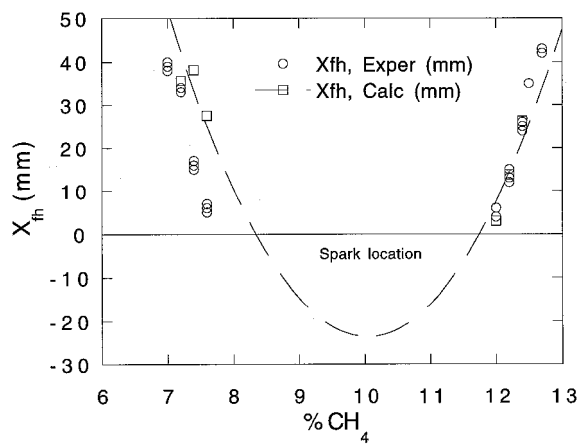

Fig. 12 Flameholding distance as a function of methane concentration. E_{spark} = 27 mJ, Um = 112 ± 5 cm/s. Note that x_{fh} = 0 is the location of the spark. The top of the burner was approximately 2 cm below this value. Methane concentrations between 7.6–12.0% by volume led to burner stabilized flames. However, the curve illustrates the predicted dependence of the flameholding distance on a mixture ratio over the full range of values.

To determine if the discrepancy between measured and calculated flameholding distances was caused by the interaction between the flame kernels, we measured the position of the lower edge of kernel 1 and the upper edge of kernel 2 as a function of time (see Fig. 2 for the definition of kernels 1 and 2). Figure 11 shows a plot of these data for the 12.2% methane gas mixture and spark energy of 27 mJ. Our model predicts that the point of intersection of the lines representing the position of these two flame fronts should be the flameholding distance. However, we find from our images that the flameholding distance lies slightly beyond this intersection point. The figure shows that as the upper edge of kernel 2 nears the lower edge of kernel 1, kernel 1 accelerates to match the speed of kernel 2. Because kernel 2 is made up of hot, burned gas, it is possible that it heats up and consequently accelerates the flow just above it. This acceleration pushes kernel 1 above its expected location. This effect may account for the systematic

underprediction of the flameholding distance by our model (Fig. 9).

Within the experimental uncertainties, the model does show good agreement with the measured flameholding positions over the limited range of pulse frequencies accessible in this experiment. It would be useful to test the model at higher frequencies that would be needed in a real device. In the limit of very high-pulse frequency, the flameholding distance approaches zero, and the flameholding behavior approaches the limit of cw spark flameholding. As pulse frequency increases, the required average laser power increases, and this may pose practical limits on the application of pulsed lasers to flameholding.

Methane Concentration Effect

The methane concentration varied from 7 to 12.7%, by volume. For methane concentrations between 7.7–11.9%, the burning velocity rose above the maximum flow speed obtainable from the flow controllers and, thus, the flame stabilized on the burner. Because the burner, not the spark, was the method of flameholding, we were unable to obtain data for this range of methane concentrations. The flameholding distance was measured at nine concentrations, and the results are shown in Fig. 12. In the experimentally accessible concentration range, we found that the flameholding distance decreases with increasing CH_4 concentration for lean ($[CH_4] < 9.5\%$) mixtures, and it increases for rich ($[CH_4] > 9.5\%$) mixtures. Our model predicts this trend based on the same trend in flame speeds.

Figure 12 also shows the calculated flameholding distance as a function of methane concentration. The calculated points were found in an analogous fashion to those in Fig. 9, using $r(t)$ curves for each CH_4 concentration. The curve drawn through the calculated points shows the extrapolated flameholding distance if no burner were present (as is the case in a combustion chamber). We see that the minimum flameholding distance occurs when the methane concentration is 10% or ϕ 1.06. This concentration corresponds to the peak laminar flame speed for methane, which indicates that the extrapolated curve is likely a good representation of the behavior in this region.[7]

Discussion

Our model and data indicate that, of the parameters investigated here, the flameholding distance is most sensitive to the flame speed. In a practical device, increasing the flame speed would then be the simplest means of increasing the performance, i.e., reducing the flameholding distance, of a pulsed laser-induced spark flameholder. Changing the fuel type, mixture ratio, and flow condition can increase flame speed. However, the flame speed cannot be increased arbitrarily and is limited in practical devices to that of stoichiometric hydrogen/air combustion. As we have shown, if the flameholding takes place within ~2.0 ms of the laser pulse, the spark energy can also play a significant role in determining the effective flame speed. This effect also appears to be limited, with relatively small gains at spark energies above 60 mJ.

Holding a flame in a hypersonic flight vehicle engine requires that the flame be maintained in a flow stream moving more than 10^4 times faster than that in this experiment. The effects of spark energy and methane concentration on the flameholding distance are expected to be largely independent of flow speed, in the absence of turbulence. Therefore, the only way to decrease the flameholding distance (and, thus, achieve a reasonable combustor length) in such a fast flow is by increasing the laser pulse frequency. Using our derived velocity profile for 12.0% methane and 27-mJ spark energy (our highest calculated velocity), we can use Eqs. (4) and (5) to predict the pulse frequency required for flameholding as a function of Mach number, assuming a flameholding distance of 10.0 cm (Fig. 13). The solid curve in Fig. 13 shows the pulse frequency needed to maintain the flame in CH_4/air, based on our experimentally obtained values. In the hypersonic region, the pulse frequency needed is on the order of 100 kHz. Lasers do exist in this pulse frequency range; however, their pulse energies are not high enough to form a spark or ignite the gas. Even if a pulsed laser could provide the needed pulse energy, the average power required for such a laser would be in the kilowatt range. At this power level, a cw laser might be more efficient and would produce a true, continuous flame. The turbulence present in a real engine, and not in our experiment, would increase the effective flame speed. For comparison, we will assume an increase of a factor of 10 over the laminar flame speed and ignore other possible effects of turbulence on flameholding, such as rapid strain and variable mixture ratio. The long-dash curve in Fig. 13 shows the pulse frequency requirements for a more turbulent CH_4/air. The required laser pulse rates are on the order of 10 kHz, which is again too high for current pulsed laser technology. If the fuel were hydrogen, a more likely choice for a high-performance vehicle and a turbulent flow were maintained, then the burning velocity could be increased 100-fold over the CH_4/air velocities found here. The short dash curve shown in Fig. 13 gives the frequency profile for this case. Note that in all of these cases, the flameholding must take place in <2 ms, and thus, the performance could be somewhat enhanced by increasing the spark energy. Currently available air-cooled, diode-pumped Nd:YAG lasers are capable of producing the kilohertz pulse rates required for turbulent H_2/air combustion, with pulse energies sufficient to produce sparks and maintain combustion in a low turbulence environment. Thus, this simple extrapolation indicates that pulsed laser-induced spark flameholding may be a feasible alternative for high-speed vehicles.

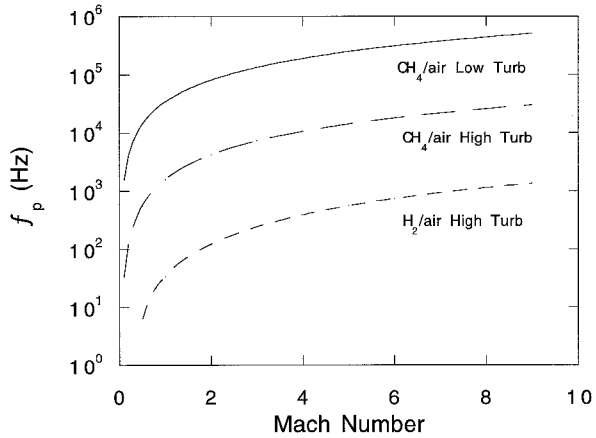

Fig. 13 Calculated pulse frequency required for flameholding as a function of Mach number. Curves were obtained using the simple flameholding model developed here and scaling of the experimental flame speed data (see text for details).

The conditions in a real engine are quite different from our simple demonstration experiment and could reduce the effectiveness of laser flameholding. For instance, the flow speed could become high enough that the gas volume illuminated by the laser moves out of the beam waist during the pulse. For typical pulsed lasers with pulse durations of <10 ns and a beam waist of ~100 μm, a flow speed >10,000 m/s would be required for this effect to become important. As noted earlier, the turbulence present in a real engine can help the flameholding process by increasing the effective flame speed; however, turbulence will also produce variable strain rates and mixture ratios that may hinder laser flameholder performance. Previous work has shown that minimum ignition energies for electric-discharge sparks increase with increasing turbulence intensity.[17] Thus, higher pulse energies may be required for reliable flameholding in turbulent flows. Additional studies will be required to determine quantitatively how turbulence effects will modify the laser pulse energy and repetition rates required for laser flameholding.

As technology advances, it may prove more desirable to use cw lasers for flameholding. This class of lasers has generally been ruled out because the high power required to maintain breakdown could only be achieved with large, inefficient gas lasers. However, recent advances in diode laser arrays promise to make high-power, compact, solid-state, cw lasers available. As larger and more efficient arrays are produced, it should be possible in the near future to produce cw sparks from solid-state cw lasers. A cw spark would provide the highest reliability and would allow operation over the widest range of flow speeds and mixture ratios.

Conclusions

Flameholding in the supercritical, subsonic flow of methane/air using pulsed laser-induced sparks was demonstrated. For spark energies between 27–60 mJ, increasing the spark energy decreases the flameholding distance. Higher spark energies lead to an increase in the flameholding distance under some conditions. Increasing the laser pulse frequency decreases the flameholding distance. As the methane/air mixture approaches the stoichiometric value, the flameholding distance drops significantly, correlating with the rise in flame speed. The smallest flameholding distance occurs at $\phi = 1.06$, the point of highest flame speed. A simple model of pulsed, laser-induced spark flameholding was presented and shown to agree well with the experimental observations. The model predicts that for H_2-fueled, hypersonic vehicles, current pulsed-laser technology may allow the use of laser-induced spark flameholding. To better understand the performance of laser flameholding in real engines, additional studies are needed to investigate the effects of turbulence on the required laser pulse energy and pulse repetition rate. Current cw-laser technology could possibly support laser-induced spark flameholding in hypersonic vehicles. Advances in laser technology are making laser-induced spark flameholding a feasible alternative for supersonic and hypersonic combustion.

Acknowledgments

The Aerospace Sponsored Research Program of the Aerospace Corporation supported this research. The contributions of one of the authors (L.D.M.) were supported by the U.S. Air Force through the Education with Aerospace Program. The authors wish to thank Jack A. Syage, Lee K. Johnson, and Paul D. Ronney for many helpful discussions.

References

[1]Ronney, P. D., "Laser Versus Conventional Ignition of Flames," *Optical Engineering*, Vol. 33, No. 2, 1994, pp. 510–521.

[2]Forch, B. E., and Miziolek, A. W., "Ultraviolet Laser Ignition of Premixed Gases by Efficient and Resonant Multiphoton Photochemical Formation of Microplasmas," *Combustion Science and Technology*, Vol. 52, Nos. 1–3, 1987, pp. 151–159.

[3]Forch, B. E., and Miziolek, A. W., "Laser-Based Ignition of H_2/O_2 and D_2/O_2 Premixed Gases Through Resonant Multiphoton Excitation of H and D Atoms near 243 nm," *Combustion and Flame*, Vol. 85, Nos. 1–2, 1991, pp. 254–262.

[4]Miziolek, A. W., and Sausa, R. C., "Photochemical Ignition Studies: I. Laser Ignition of Flowing Premixed Gases," Ballistic Research Lab., TR-2644, Aberdeen Proving Ground, MD, 1985.

[5]Chou, M. S., and Zukowski, T. J., "Ignition of H_2/O_2/NH_3, H_2/Air/NH_3 and CH_4/O_2/NH_3 Mixtures by Excimer-Laser Photolysis of NH_3," *Combustion and Flame*, Vol. 87, No. 2, 1991, pp. 191–202.

[6]Maus, U., Raffel, B., Wolfrum, J., and Warnatz, J., "Observation and Simulation of Laser Induced Ignition Processes in O_2-O_3 and H_2-O_2 Mixtures," *21st Symposium (Intenational) on Combustion*, Combustion Inst., Pittsburgh, PA, 1986, pp. 1869–1876.

[7]Lavid, M. Poulos, A. T., Gulati, S. K., Nachshon, Y., and Stevens, J. G., "Excimer Laser Relight for the Supersonic Commercial Transport Aircraft," *SPIE*, Vol. 1862, 1993, pp. 59–70.

[8]Lefebvre, A. H., *Gas Turbine Combustion*, Hemisphere, Washington, DC, 1983, pp. 33–72.

[9]Fendell, F. E., Kung, E. Y., and Sheffield M. W., "Flame Configuration Associated with Localized Energy Addition to a Flowing Combustible Mixture," *AIAA Journal*, Vol. 8, No. 2, 1992, pp. 464–471.

[10]Hill, P. G., and Peterson, C. R., *Mechanics and Thermodynamics of Propulsion*, 2nd ed., Addison–Wesley, Reading, MA, 1992, pp. 155–164, 246–268.

[11]Raizer, Y. P., *Laser-Induced Discharge Phenomena*, Consultants Bureau, New York, 1977, pp. 63–103, 274–284.

[12]Grey-Morgan, C., "Laser-Induced Electrical Breakdown of Gases," *Electrical Breakdown of Gases*, edited by J. M. Meek and J. D. Crags, Wiley, New York, 1978, pp. 717–752.

[13]Syage, J. A., Fournier, E. W., Rianda, R., and Cohen, R. B., "Dynamics of Flame Propagation Using Laser-Induced Spark Initiation: Ignition Energy Measurements," *Journal of Applied Physics*, Vol. 64, No. 3, 1988, pp. 1499–1507.

[14]Spiglanin, T. A., McIlroy, A., Fournier, E. W., Rianda, R., Cohen, R. B., and Syage, J. A., "Time-Resolved Imaging of Flame Kernels: Laser Spark Ignition of H_2/O_2/Air Mixtures," *Combustion and Flame*, Vol. 102, No. 3, 1995, pp. 310–328.

[15]Smith, D. C., and Fowler, M. C., "Ignition and Maintenance of a cw Plasma in Atmospheric-Pressure Air with CO_2 Laser Radiation," *Applied Physics Letters*, Vol. 22, No. 10, 1973, pp. 500–502.

[16]Fendell, F. E., Chow, M. S., Zukowski, T. J., and Carrier, G. F., "Initiation and Modification of Reaction by Energy Addition: Kinetic and Transport Phenomena," Air Force Office of Scientific Research, TR 90-1140, 1990.

[17]Lefebvre, A. H., "Basic Ignition Research Related to Altitude Relight Problems," *Gas Turbine Combustor Design Problems*, edited by A. H. Lefebvre, Purdue Univ., West Lafayette, IN, 1978, pp. 189–201.